Effects of granular additives on transition boundaries between flow states of rimming flows

O. A. M. Boote and P. J. Thomas[a)]
Fluid Dynamics Research Centre, School of Engineering, University of Warwick, Coventry CV4 7AL, United Kingdom

(Received 20 September 1998; accepted 27 April 1999)

An experimental study of the rimming flow established inside a partially fluid-filled cylinder rotating around a horizontal axis of rotation is described. For the first time effects of granular additives on transition boundaries between flow states adopted by the fluid for different experimental conditions are studied. For the granule-free fluid and low filling levels we confirm results of previous authors showing that the ratio of viscous stresses and gravitational force remains constant along the transition boundaries considered. For higher filling levels our new data indicate, however, that the gravitational force becomes increasingly more important. For the solid–liquid two-phase flow our data reveal that even small amounts of granular additives can have a significant effect on a suitable parameter defined to characterize the transition boundaries. Granular additives can lead to the stabilization of states and to the extension of the parameter range over which certain states can be observed. It is shown that the origin of the observed effects appears to be associated with an increased bulk density of the solid–liquid flow. For high granule concentrations a pattern of equally-spaced circumferential granular bands is observed to form on the inner cylinder wall. It is speculated that these bands form as a consequence of the mechanism which has been referred to as shear-induced migration/diffusion in the literature in the past. It appears that the granule-band pattern has not been observed previously for the flow investigated here. © *1999 American Institute of Physics.* [S1070-6631(99)04508-0]

I. INTRODUCTION

We consider one example of a general group of flows conventionally classified as coating flows. The particular example studied here is the flow established inside a partially fluid-filled cylinder which rotates around a horizontal axis of rotation. While the cylinder rotates fluid is dragged up and around the inner cylinder wall. This flow is usually referred to as a rimming flow. Depending on the rotation rate, the filling level and the fluid properties, various distinct and easily observable flow patterns can be displayed by the fluid inside the cylinder. Such a formation of a variety of different patterns is a typical feature shared by many coating flows. The flow patterns, or flow states, of the rimming flow reveal themselves as relatively simple, stationary or nonstationary, flow structures in some cases and as very complex patterns in others. The majority of patterns adopted are, however, markedly distinct from each other and most of them are relatively easy to reproduce. Any two flow states are, generally, separated from each other by a well-defined, state-transition boundary. These features make the rimming flow an ideal paradigm for the study of some questions associated with fundamental problems in fluid dynamics. In recent years this flow has, for instance, been the scope of interest in the context of research involved with pattern-formation phenomena on one-dimensional fronts, as well as in the context of studies concerned with transition to spatio-temporal chaos (Melo,[1] Melo and Douady,[2] Vallette, Edwards, and Gollub,[3] Vallette, Jacobs, and Gollub[4]). However, the rimming flow and coating flows in general, also appear frequently in industrial applications. Therefore they evidently bear significant relevance to numerous topics in applied engineering science (Karapantsios *et al.*,[5] Benkreira *et al.*,[6] Wilhelmson *et al.*,[7] Chew[8]).

It appears that topics related to the rimming flow were first considered in the literature by White,[9] White and Higgins,[10] and Phillips.[11] The first study focusing on the actual flow patterns adopted by the flow appears in the work of Balmer[12] who summarizes briefly some qualitative results of an experimental investigation. Surprisingly, however, Balmer only describes one single example of the variety of flow patterns which can indeed be displayed by the flow. Probably the most complete and in-depth description to date of the various flow states associated with the rimming flow has very recently been published by Thoroddsen and Mahadevan.[13] Their paper also contains what appears to be a fairly comprehensive overview of the relevant literature on the subject so that we will refrain from repeating a similar summary here. We would, however, like to add two further publications to this summary. The first of these publications is by Sanders, Joseph, and Beavers[14] who appear to be the only authors who consider fundamental aspects of the rimming flow for a non-Newtonian fluid. The second, very recent, publication is by Hosoi and Mahadevan.[15] These authors describe a linear numerical stability analysis and

a)Author to whom correspondence should be addressed. Electronic mail: pjt@eng.warwick.ac.uk

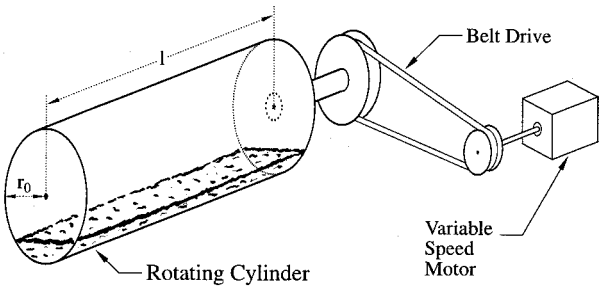

FIG. 1. Sketch of the experimental set-up.

present new results for the axial instability of the free-surface front.

The purpose of the present paper is to document first results associated with an aspect of the flow which, to our knowledge, has not been considered previously in the existing literature. The question addressed concerns the effects of small, granular additives on the state-transition boundaries between different flow states displayed by the rimming flow. We will also document, for the first time, the observation a new pattern developing in the flow when the fluid contains a sufficiently high concentration of granules. The main goals of our ongoing research are to determine how and to ultimately understand the physical mechanisms whereby successive increases of the granule concentration modify the flow states and, in particular, the transitions between different states in coating flows.

It is well known[16] that under certain conditions the flow of solid–liquid suspensions can be described by appropriate bulk fluid properties. Here we will attempt to determine if evidence exists which would allow us to attribute any influences of granular additives on state-transition boundaries of the rimming flow to modifications of bulk fluid properties such as the bulk viscosity or the bulk density. Although we approach the flow from a fundamental viewpoint it is evident that the results of our research will be of interest, for instance, in the context of applications involving mixing in solid–liquid suspension flows in the food, pharmaceutical or processing industry.

II. EXPERIMENTAL SETUP AND METHODS

Our experiments were carried out employing an apparatus which is, in principle, very similar to those used in previous related studies. A sketch of the apparatus is shown in Fig. 1. The facility consists, briefly, of a hollow, transparent cylinder with an inner radius of $r_0 = 5.00 \pm 0.01$ cm and a length $l = 27.0$ cm which rotates with an angular velocity ω around a horizontal axis of rotation. The cylinder is manufactured from Acrilite (Blanson Ltd., Leicester) which is a material enabling an exceptionally high-clarity viewing of the flow behavior through the cylinder wall.

For the experiments the cylinder is partly filled with an amount of fluid of volume V. The cross-sectional area of the cylinder occupied by the fluid is thus $A = V/l$. The filling fraction of the cylinder is defined as A/A_0 with $A_0 = \pi r_0^2$ representing the total cross-sectional area of the cylinder.

The cylinder is rotated by a variable-speed 12 V dc motor via a belt-drive mechanism as indicated in Fig. 1. By means of a manual speed controller the rotational frequency f of the cylinder can be adjusted between $0\,\mathrm{Hz} < f < 4.7\,\mathrm{Hz}$. For low angular velocities the rotation rate was determined by measuring the time required for a certain number of cylinder rotations by means of a stopwatch. For higher rotational speeds, whenever it was not possible to reliably count the number of cylinder rotations, the rotational frequency was measured by means of a handheld, mechanical tachometer. The measuring accuracy of the tachometer is ± 1 rpm. The rotational velocity of the cylinder is expressed in terms of a Reynolds number Re defined as

$$\mathrm{Re} = \frac{\omega r_0 h}{\nu}. \tag{1}$$

where

$$h = \frac{V}{2\pi r_0 l} \tag{2}$$

represents a measure for the mean thickness of the coating on the inner wall of the cylinder.

The fluid used is silicone fluid (Ambersil, F111/500). The manufacturer's data sheet states that the density of the silicone fluid is $\rho_F = 0.973\,\mathrm{g\,cm^{-3}}$ and that its kinematic viscosity is $\nu = 5.0\,\mathrm{cm^2\,s^{-1}}$ at 25 °C. These values represent with sufficient accuracy the properties of the silicone fluid during the experiments when its temperature was approximately 21 ± 1 °C.

The granular material added to the silicone fluid are spherical glass beads (Potters-Ballotini, Spheriglass 1619 grade CP00). We have measured the density of the beads as $\rho_G = (2.500 \pm 0.003) \times 10^3\,\mathrm{kg\,m^{-3}}$. The manufacturer's data sheet states that the diameter d_G of 90% of the beads lies in the interval between 250 μm and 425 μm.

From a balance of Stokes drag, gravitational force and buoyancy force one can determine the settling velocity V_S of the granules in the pool of silicone fluid in the cylinder as $V_S = (d_G^2\, g/18\mu) \cdot (\rho_G - \rho_F)$. For the present experiment one estimates that V_S is of the order of $0.015\,\mathrm{cm\,s^{-1}}$. The turnover of the fluid in the pool proceeds on a typical velocity scale given by $V_T = \omega r_0$. For the present experiments this velocity is in the range of $0.94\,\mathrm{cm\,s^{-1}} < V_T < 148\,\mathrm{cm\,s^{-1}}$. From this one gets $63 < V_T/V_S < 9870$. Hence, the typical flow velocities are between two and four orders of magnitude larger than the settling velocity of the glass beads. On the basis of these consideration one expects that the beads will remain uniformly mixed throughout the fluid as long as no additional mechanisms are activated which result in granule segregation.

We specify the amount of granular material introduced in the liquid by the granule mass M which is added per cubic centimeter of silicone oil. We also refer, interchangeably, to the amount of granules added in terms of a quantity defined on the basis of the liquid volume ΔV which the granules displace. The displaced volume ΔV is given by

$$\Delta V = l \cdot \Delta A = \frac{MAl}{\rho_G}, \tag{3}$$

where ΔA is the associated change of the cross-sectional cylinder area occupied by the fluid. The modified cross-sectional area A_m of the cylinder which is occupied by the mixture of fluid and granules together is then

$$A_m = A + \Delta A = A \cdot \left(1 + \frac{M}{\rho_G}\right). \tag{4}$$

The modified filling fraction A_m/A_0 as a result of adding granular material is thus

$$\frac{A_m}{A_0} = \frac{A}{A_0} \cdot \left(1 + \frac{M}{\rho_G}\right). \tag{5}$$

We will generally refer to the amount of granules added in terms of this modified filling fraction. It is advantageous to use this quantity as it provides one with a better feel for the two properties (the granule mass per unit volume of liquid and the filling level of the cylinder) which are necessarily changed simultaneously when adding a certain amount of granules to the fluid.

As a consequence of the addition of granules to the fluid the mean thickness of the coating on the inner wall of the rotating cylinder also changes. The modified mean thickness h_m is obtained by replacing the volume V in Eq. (2) by $V + \Delta V$. Correspondingly, an associated modified Reynolds number Re_m is then obtained by replacing the height h in Eq. (1) by h_m. As will be seen it is not necessary to account for a modified viscosity to calculate Re_m whenever this modified Reynold number is employed in the context of the particular issues addressed here.

III. EXPERIMENTAL RESULTS

A. Flow patterns in the system free of granules

Figure 2 shows a sequence of photographs which illustrate the main flow states dealt with throughout the remainder of this paper. The scale of the pictures can be inferred through the cylinder length $l = 27$ cm which corresponds approximately to the width horizontally across each picture. The photographs displayed were obtained from an experiment for which the rotating cylinder was partly filled with silicone fluid free of granular additives. The figure primarily serves to define the terminology adopted here which is required to follow the discussion of our results. Nevertheless, we have not repeated a visualization of the trivial state, the flat-front state, in our Fig. 2. If required the reader is asked to refer to Fig. 3(a) of Melo[1] to view a visualization of this state. The various flow patterns will be referred to as indicated in the caption of Fig. 2. The flow visualizations shown are qualitatively very similar to corresponding photographs by other authors (Melo,[1] Thoroddsen and Mahadevan[13]) obtained under comparable experimental conditions. Figure 2 is not intended to give a comprehensive overview of all the possible flow states that can be displayed by the system. For such an overview the reader is referred to the article by Thoroddsen and Mahadevan[13] and the references contained therein.

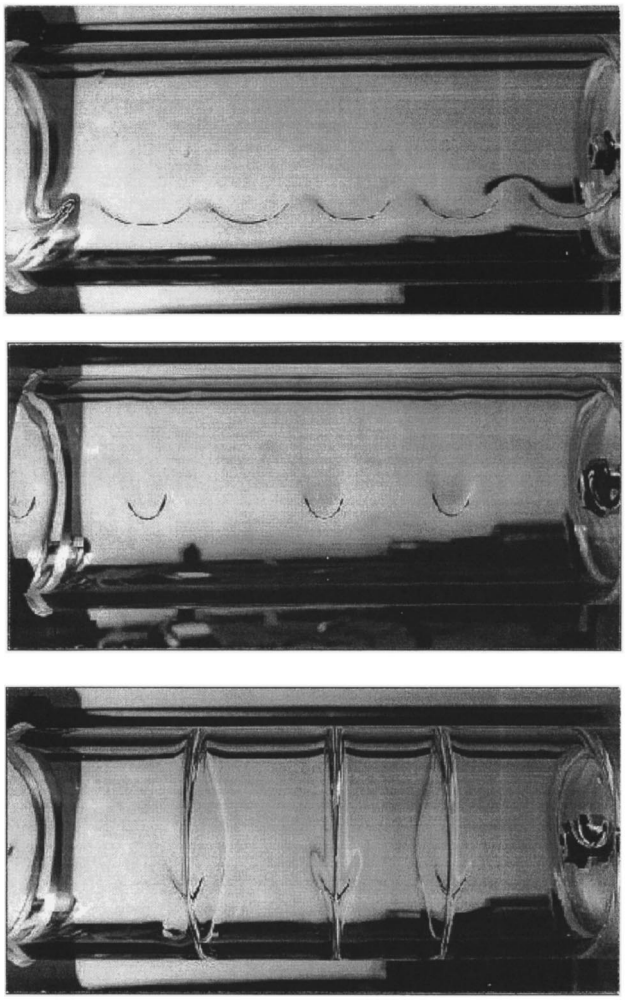

FIG. 2. Visualizations of flow states displayed by the granule-free system for a filling fraction of $A/A_0 = 0.144$. (a) Modulated front, $\omega \approx 8.7\ \mathrm{rad\ s^{-1}}$, $\mathrm{Re} \approx 3.1$. (b) Localized structures, $\omega \approx 9.4\ \mathrm{rad\ s^{-1}}$, $\mathrm{Re} \approx 3.4$. (c) Hydrocysts, $\omega \approx 11.5\ \mathrm{rad\ s^{-1}}$, $\mathrm{Re} \approx 4.2$

B. Flow patterns in the system containing granules

As long as the amount of granular material introduced in the system remains below a certain critical concentration all transitions between flow patterns observed in the granule-free system appear in qualitatively similar form in the system containing granular additives. However, as will be seen later, even small granule concentrations can affect the fluid dynamics through measurable influences on the state-transition boundaries.

For low granule concentrations we have observed that the granules remain approximately uniformly distributed throughout the fluid at all times. This is consistent with our brief theoretical considerations in Sec. II concerning this matter. However, for granule concentrations above a critical value of $M_c \approx 0.12\ \mathrm{g\ cm^{-3}}$ (corresponding to $A_m/A \approx 1.048$ or $A_m/A_0 \approx 0.15$) the flow displays a qualitative difference. This difference is illustrated by the photographs in Figs. 3(a)–3(c). The experiments have shown that above concentrations of M_c a pattern of equally-spaced circumferential bands forms on the inner cylinder wall. This pattern is a result of granule accumulations at certain locations along the

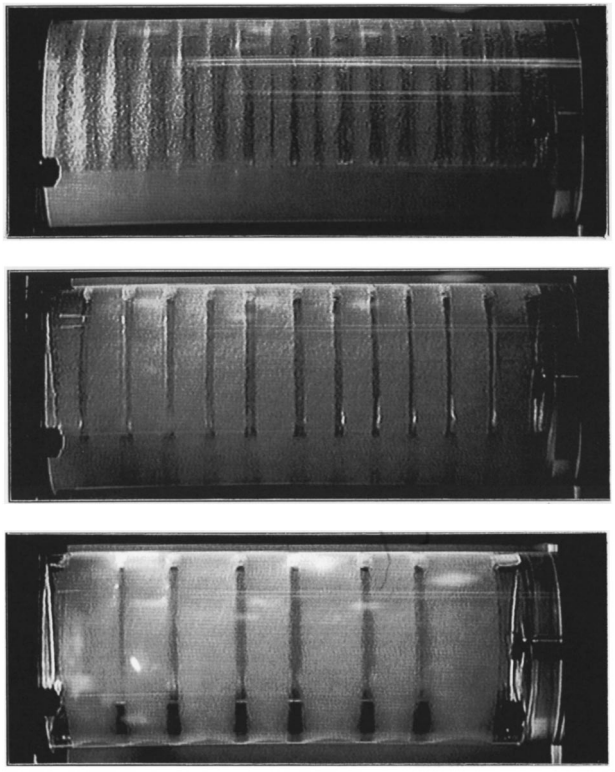

FIG. 3. Visualizations showing the granule-band structure which develops above the critical granule concentration of $M_c \approx 0.12\ \mathrm{g\,cm^{-3}}$. The photographs shown were obtained for $M \approx 0.33\ \mathrm{g\,cm^{-3}}$ (corresponding to $A_m/A_0 \approx 0.151$). The wavelengths λ and the angular velocities associated with the photographs are (a) $\lambda \approx 1.7$ cm, $\omega = 0.33$ rad/s, (b) $\lambda \approx 2.3$ cm, $\omega = 1.68$ rad/s, (c) $\lambda \approx 3.9$ cm, $\omega = 3.67$ rad/s.

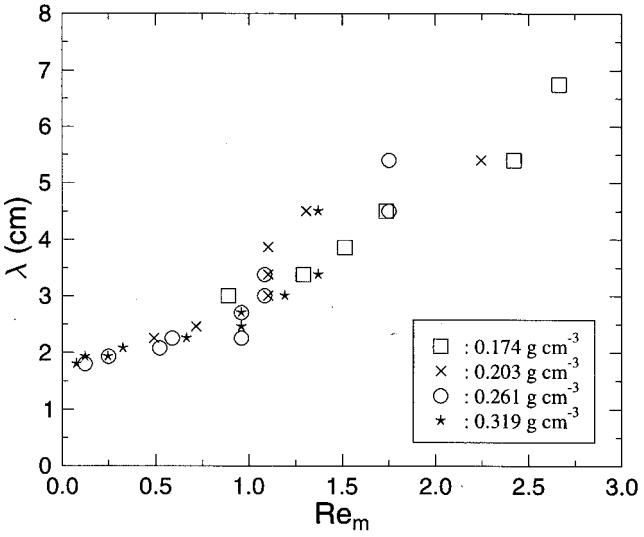

FIG. 4. Wavelength λ of the granule-band structure as a function of the Reynolds number Re for four different granule concentrations M.

span of the cylinder. The pattern develops if the cylinder is left to rotate undisturbed for a few minutes. Neighboring granular bands are separated from each other by a narrow region of fluid which is almost free of granules. The angular velocity of the cylinder at which the granular bands first form decreases with an increasing granule concentration in the fluid. For higher granule concentrations of around $0.366\ \mathrm{g\,cm^{-3}}$ the bands were observed to occur for cylinder rotation rates as low as $f \approx 0.03$ Hz.

One can estimate the value of the modified dynamic viscosity μ_m of silicone fluid corresponding to the critical granule concentration of M_c. According to Einstein[17] (see also Soo[16]) the modified dynamic viscosity μ_m of an incompressible fluid containing solid spheres is given by $\mu_m = \mu(1 + 2.5\alpha)$ for small α, where α is the proportion of the total volume occupied by the particles. With the data provided in Sec. II one determines $\mu = 4.865\ \mathrm{g\,cm^{-1}\,s^{-1}}$ and one finds that $M_c \approx 0.12\ \mathrm{g\,cm^{-3}}$ corresponds to a value of $\alpha \approx 0.048$. With this one obtains $\mu_m \approx 5.45\ \mathrm{g\,cm^{-1}\,s^{-1}}$. This represents an increase of the the dynamic viscosity of 12% in comparison to the viscosity of the granule-free silicone fluid. With the values for the fluid and the granule density one can further determine that the bulk density associated with $M_c \approx 0.12\ \mathrm{g\,cm^{-3}}$ is $1.046\ \mathrm{g\,cm^{-3}}$. This represents an increase of approximately 7.5% in comparison to the density of the granule-free silicone fluid.

To our knowledge the formation of the granular bands shown in Fig. 3 has not been previously documented in the literature in association with the flow geometry studied here. However, the banding structure of our Fig. 3 is very similar to structures observed by Janes,[18] Janes and Thomas,[19] and recently by Tirumkudulu *et al.*[20] in horizontal Taylor–Couette systems which were partially filled with fluid containing granular additives.

In the case of the present flow geometry one might suspect that the band structure is related to the disking or hydrocyst pattern which can be observed in systems free of granules. We will argue that it is very unlikely that this is the case. The hydrocyst pattern was first documented in Fig. 1 and Fig. 2 of Balmer,[12] and in Fig. 2 of Karweit and Corrsin[21] and it has more recently also been documented in Fig. 22(a) of Thoroddsen and Mahadevan.[13] These authors report that the pattern generally occurs at higher filling fractions and at rotational frequencies of a few cycles per second. This is in agreement with our own results presented in the following section. As was already indicated granule bands form, however, at significantly lower rotational speeds and filling fractions than the hydrocysts in a granule-free system. This appears to indicate that the origins of the two somewhat similar looking patterns are not the same.

Figure 4 displays the wavelength λ of the granule-band structure as a function of the modified Reynolds number Re_m for four different concentrations M of granular additives. The data were obtained from experiments for which the initial filling fraction before the introduction of granules was $A/A_0 = 0.144$. The modified Reynolds number is based on that angular velocity ω at which each of the patterns with a certain number of bands was first observed. Once a pattern is formed it remains stable over a certain Reynolds number interval before the number of bands slowly changes again. Figure 4 suggests that there is a minimum pattern wavelength of $\lambda \approx 1.7$ cm which is approached at low Reynolds numbers. The figure shows that the wavelength increases

substantially with the Reynolds number and, hence, with the angular velocity of the cylinder.

It is noted that in the present context there is no need to account for a modified viscosity of the fluid when calculating the modified Reynolds number displayed on the abscissa of Fig. 4. Once bands begin to form a single viscosity value can, evidently, not be defined as there are simultaneously regions of high and low granule concentrations. Employing the value corresponding to the viscosity of the fluid just below the critical granule concentration M_c does, of course, result in using the same viscosity value for all four data sets of Fig. 4. This would, consequently, only rescale the x-axis slightly but it would not affect the data interpretation.

Thoroddsen and Mahadevan[13] report that hydrocyst formation in a granule-free system is initiated at the end walls. The number of structures increases with an increasing cylinder rotation rate until the entire span of the cylinder is filled with equally-spaced hydrocysts. Once this state is established the associated pattern wavelength is independent of or, at most, only weakly dependent on the rotation rate of the cylinder.[12,13,21] This is consistent with our own observations. It substantiates our earlier speculation that the granular bands, whose pattern wavelength increases substantially with the rotation rate, are unlikely to be a visualization of the hydrocyst pattern.

Nevertheless, Fig. 4 also reveals that the wavelength appears to be independent of the amount of granular material added. This would suggest that the band structure is not formed as a consequence of the granules altering the system dynamics as such. It consequently appears to suggest that the bands represent a visualization of a modified realization of a feature also present in the granule-free system. In this context it should be noted that the magnitude of the wavelength of the granule-band pattern is of the same order as the wavelength of the patterns referred to as ''sharkteeth'' and ''fishlike'' by Thoroddsen and Mahadevan[13] and which are displayed in their Fig. 10 and Fig. 16. Nevertheless, similar to the hydrocyst structure these patterns are also established at much higher angular velocities of the cylinder than the granule-band pattern. However, as is expressed by Fig. 11 of Thoroddsen and Mahadevan[13] the wavelength of the sharkteeth pattern increases with the angular velocity of the cylinder, like the granule-band wavelength, at least in a certain velocity interval.

Our observations appear to have shown that granule-band formation is initiated while the fluid in the cylinder is in a flat-front state. Upon increasing the cylinder speed a distinct modulated front is observed to develop. The centers of the (already developed) granular bands then each coincide with the location of a wave crest on the modulated front as is illustrated in Fig. 5(a). When the cylinder velocity is increased further the modulated front breaks down. The troughs of the modulated front then develop into stationary, U-shaped structures as displayed in Fig. 5(b). These U-shaped structures are similar to the structures shown in Fig. 2(b) for a granule-free fluid. Upon further increasing the angular velocity the U-shaped structures subsequently develop into patterns very similar to the hydrocysts in granule-free systems which are shown in Fig. 2(c).

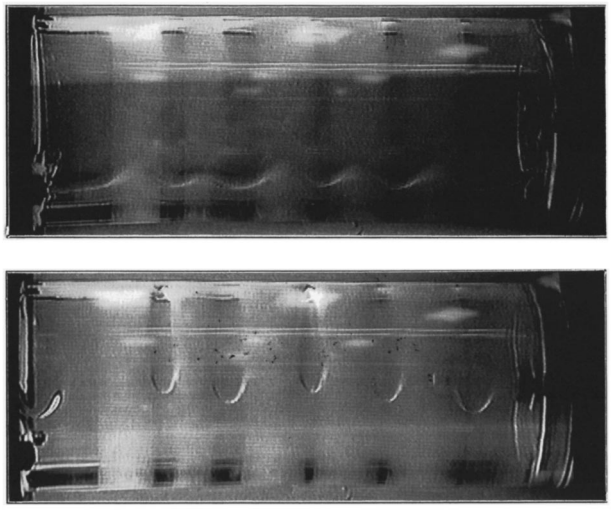

FIG. 5. Visualizations showing (a) modulated-front state in a system containing granules, $\omega = 6.6$ rad/s, (b) localized, stationary U-shaped structures between granule bands, $\omega = 8.2$ rad/s, for a relatively low granule concentration of the order of $M \simeq 0.174\ \mathrm{g\,cm^{-3}}$ and an initial filling fraction of around $A/A_0 \simeq 0.13$.

It was not possible to decide if it is the flow prior to the development of the modulated front which initially gives rise to the formation of the granular bands and, hence, determines their number and fixes their spatial position. Alternatively, the granular bands might, following the initiation of their formation, result in a modulated-front state which is indeed a different state than the one observed in the granule-free system. It is interesting to note that a certain type of modulated-front state with evidence of some cell structure has also been observed very recently by Fried, Shen, and Thoroddsen[22] in a rotating cylinder which only contains granules and no fluid whatsoever.

With regard to the discussion of Tirumkudulu *et al.*[20] it would, in summary, appear that the granule-band pattern observed in our experiment has a similar origin as the structures developing in their horizontal Taylor–Couette system. Tirumkudulu *et al.* attribute the band formation in their system to the mechanism which has been referred to as shear-induced migration/diffusion by Leighton and Acrivos.[23] By this mechanism particles are assumed to migrate from regions of high shear to regions with low shear and from regions with high particle concentrations to regions with low concentrations. However, as the main concern of this paper is not the granule-band structure we will not elaborate here any further on this feature of the flow.

C. State-transition boundaries in the system free of granules

Before commencing to determine the influence of granular additives on the state-transition boundaries it is necessary to ascertain that our experimental facility is indeed suitable to reproduce with sufficient accuracy results previously obtained by other researchers. In order to verify this we compare our results with the results of Melo.[1] Melo has carried out a study under experimental conditions closely matching

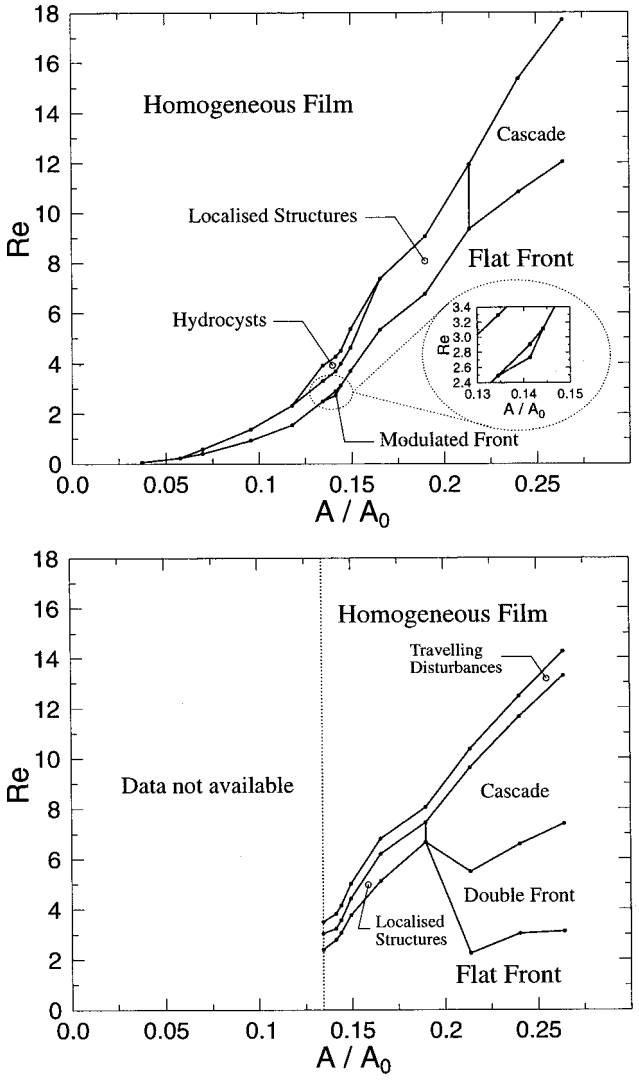

FIG. 6. State diagrams for the transition between different flow states when the cylinder is filled with silicone fluid free of granular additives. The rotational speed is (a) increased from rest (b) decreased from initially high rotation rates by a sequence of successive small increments.

those of the present investigation. He used a cylinder with the same diameter as the one used here and a silicone fluid with the same viscosity as the fluid used during the present experiments.

Figures 6(a) and 6(b) show state diagrams for the transition between different flow states when the cylinder is filled with silicone fluid which is free of granular additives. The two figures correspond to experiments during which the angular velocity was, respectively, increased and decreased by a succession of small increments. The time interval between two successive velocity changes was, as in the case of Melo's study, of the order of 30 rotation periods or longer.

From the data provided by Melo[1] it is possible to calculate the value of the Reynolds number, as defined here in Eq. (1), for the flow states shown in his Fig. 3 and Fig. 4. For Melo's Figs. 3(a)–3(c), which corresponds to a filling fraction of $A/A_0=0.136$, one finds (a) Re=2.35, (b) Re=2.49, and (c) Re=2.55. Accordingly one finds for his Figs. 4(a)–4(c), which corresponds to a filling fraction of $A/A_0=0.182$, values of (a) Re=5.51, (b) Re=5.94, and (c) Re=6.58. With reference to these Reynolds numbers and to Melo's Fig. 3 it can be seen that the transition from the flat-front state via the modulated-front state to the state displaying localized structures has occurred over a very narrow Reynolds number interval of $\Delta\,\mathrm{Re}\approx 0.2$. This is in very good quantitative agreement with the behavior observed in the present experiment as becomes evident from the data displayed in our Fig. 6(a) for filling fractions in the interval of $0.135\leqslant A/A_0\leqslant 0.145$. It is emphasized that it is not a simple matter to adjust the system parameters such that the modulated front state is displayed as the parameter regime over which the state occurs is so narrow.

For filling fractions above approximately $A/A_0=0.145$ (corresponding to $A^2\approx 130\,\mathrm{cm}^4$ in Melo's notation) we have observed that the flat-front state changes into the state displaying localized structures without initially adopting the intermediate state characterized by the modulated front. The data displayed in Melo's Fig. 2 reveal that the same behavior occurred in his system. This is expressed in his figure by the boundary located at $A^2\approx 190$ (corresponding to $A/A_0\approx 0.176$ in the present notation) which separates regions 2 and 3 of his figure.

In order to facilitate a more quantitative comparison between the overall fluid dynamics of Melo's[1] and the present system we will analyze our data analogous to the procedure followed by him. The results of this analysis can then be compared to the data of Melo's Fig. 2. Following Melo and other previous authors[24,25] we define a dimensionless parameter Λ as

$$\Lambda=\frac{C}{\epsilon\,\mathrm{Re}}=\frac{\omega r_0\nu}{gh^2}. \tag{6}$$

In Eq. (6) $C=\omega^2 r_0/g$ characterizes the ratio of centrifugal and gravitational force, $\epsilon=h/r_0$ identifies the filling level of the cylinder and Re is the Reynolds number as defined in Eq. (1). By means of the cross-sectional area $A=V/l$ of the cylinder occupied by fluid together with Eq. (2) one can replace h in Eq. (6) by A. This yields

$$\Lambda=\frac{(2\pi)^2\nu r_0^3\omega}{gA^2}. \tag{7}$$

With reference to Eq. (6) it can be seen that Λ characterizes the competition between viscous stress and gravitational force. Inspection of Eq. (7) shows that Λ is constant along a straight line in a plane displaying ω as a function of A^2. The equation can, thus, be employed to determine Λ experimentally. When $\omega=\omega_c$, where ω_c is the critical velocity associated with a particular state transition boundary, Λ reflects the constant force ratio of viscous stress and gravitational force for the transition considered. Hence, it is reasonable to assume that the two experimental facilities display sufficiently similar dynamics when the values of Λ for corresponding state transitions in both systems are approximately equal.

Figure 7 displays our experimental data for ω_c as a function of A^2 for three different state transitions. The data are, as in the case of Melo's[1] Fig. 2, for a decreasing angular velocity of the cylinder. The data displayed are for the tran-

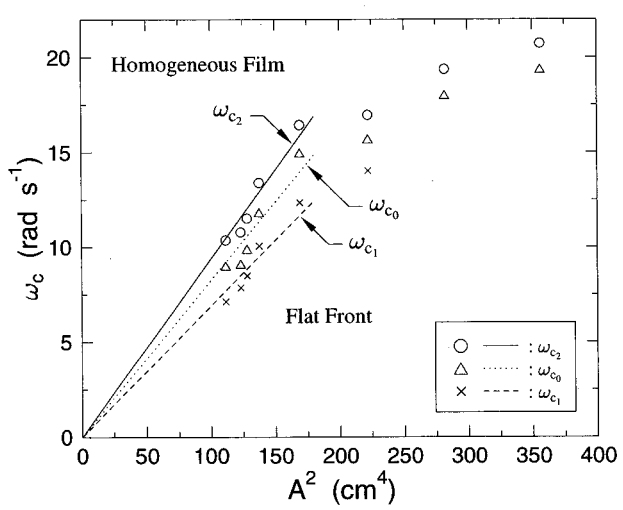

FIG. 7. Diagram showing present experimental data in a representation displaying the rotation rate ω_c of the cylinder at the point of transition as a function of A^2.

sition from the homogeneous film to the state displaying traveling disturbances (ω_{c_2}); for the transition from the traveling disturbances to the state displaying localized, stationary disturbances (ω_{c_0}); and for the transition from the flow state displaying localized, stationary structures to the flat-front state (ω_{c_1}). The flow transitions considered here and the nomenclature used are entirely analogous to the representation in Melo's[1] Fig. 2.

The lines shown in our Fig. 7 represent least-square fits through those of our data points for which $A^2 \leqslant 200\,\mathrm{cm}^4$ (corresponding to $A/A_0 = 0.180$) together with the additional necessary condition that $\omega(A^2=0)=0$. We have not included those data points in the linear least-squares fits for which $A^2 > 200\,\mathrm{cm}^4$ as Fig. 7 reveals that Λ is evidently no longer constant for filling heights above this value. From the least-squares fits one finds the following values of the parameter Λ: $\Lambda_2 = 2.36$, $\Lambda_1 = 1.74$, and $\Lambda_0 = 2.08$. The corresponding values obtained by Melo[1] are $\Lambda_2 = 2.14$, $\Lambda_1 = 1.56$, and $\Lambda_0 = 1.67$. The values of Λ_2 and Λ_1 of both experiments differ by about 10% and are, thus, in good agreement. The values for Λ_0 differ by approximately 25%. Considering the relatively limited number of data points on which the least-squares fits are based, the values of Λ_0 for both experiments show a reasonably satisfactory agreement. Consequently it appears justified to conclude that the dynamics displayed by our rotating-cylinder system are sufficiently similar to the dynamics displayed by Melo's system.

It was already indicated above that for values of $A^2 > 200\,\mathrm{cm}^4$ (corresponding to $A/A_0 > 0.18$) it is not reasonable to approximate our data points in Fig. 7 by linear least-squares fits. For filling levels above the level associated with $A^2 > 200\,\mathrm{cm}^4$ the value of Λ decreases. Melo[1] has only included two single experimental data points for one of the state transitions (ω_{c_1}) at values of $A^2 > 200\,\mathrm{cm}^4$ in his Fig. 2. As he does not comment on the behavior of the system for larger filling fractions it is not known whether his system did indeed also display the behavior observed here. We are not aware of any other data which could be used for comparison. With regard to the physical interpretation of the parameter Λ our new observation suggests that at higher filling levels transition either becomes more strongly dominated by gravitational forces or, alternatively, that it no longer depends on the interplay between viscous stresses and gravitational forces alone.

A comparison of the boundaries for the instability of the flat-front state in our Figs. 6(a) and 6(b) reveals that there is no appreciable hysteresis for $0.13 \leqslant A/A_0 \leqslant 0.19$. This corroborates similar observations reported by Melo.[1] Above $A/A_0 \approx 0.19$ the transition scenario for increasing and decreasing cylinder rotation rates is fundamentally different such that comments concerning hysteresis are not applicable. Hysteresis effects are, however, present for the stability boundaries of the homogeneous-film state in the spin-up and spin-down case. This is in agreement with the observations recently reported by Thoroddsen and Mahadevan.[13]

D. State-transition boundaries in the system containing granular additives

Melo[1] has focused in his study on the investigation of those particular state transitions which were also discussed here in the preceding section. In order to be able to quantitatively relate data obtained in a granule-free system to the corresponding behavior in a system which is modified through granules we will, in the remainder, continue to focus on these state transitions. The diagrams in Figs. 8(a) and 8(b) illustrate how increasing amounts of granular additives influence transition boundaries between these states. Figures 8(a) and 8(b) display, respectively, results obtained for the state-transition boundaries for the case of increasing and decreasing angular velocities of the cylinder.

In Figs. 8(a) and 8(b) the amount of granules added is expressed, according to Eq. (5), in terms of the modified filling fraction A_m/A_0. The ordinate displays the associated modified transitional Reynolds number Re_m defined as described at the end of Sec. II. For low granule concentrations the modified Reynolds number should here, strictly, be based on the modified bulk viscosity[16,17] of the fluid which is attained following the addition of the granules. However, for the larger concentrations above $A_m/A_0 = 0.15$, when granule band formation is initiated, it is not possible to uniquely define such a modified viscosity. The viscosity value of the granule-free fluid was, thus, used to calculate the values of Re_m in Figs. 8(a) and 8(b). This makes it necessary to interpret Re_m, in the context of this figure, as merely the nondimensionalized rotational velocity of the cylinder.

The data points for $A_m/A_0 = A/A_0 = 0.144$ in Figs. 8(a) and 8(b) correspond to the transitional Reynolds numbers for this particular filling fraction for the granule-free liquid. The initial filling fraction of $A/A_0 = A_m/A_0 = 0.144$ was chosen because it is located, with regard to Fig. 6(a), within that parameter range in which the most interesting dynamics can be expected.

The addition of a certain amount of granules necessarily results in an associated change of the filling fraction. Consequently, Fig. 8 cannot unambiguously distinguish between

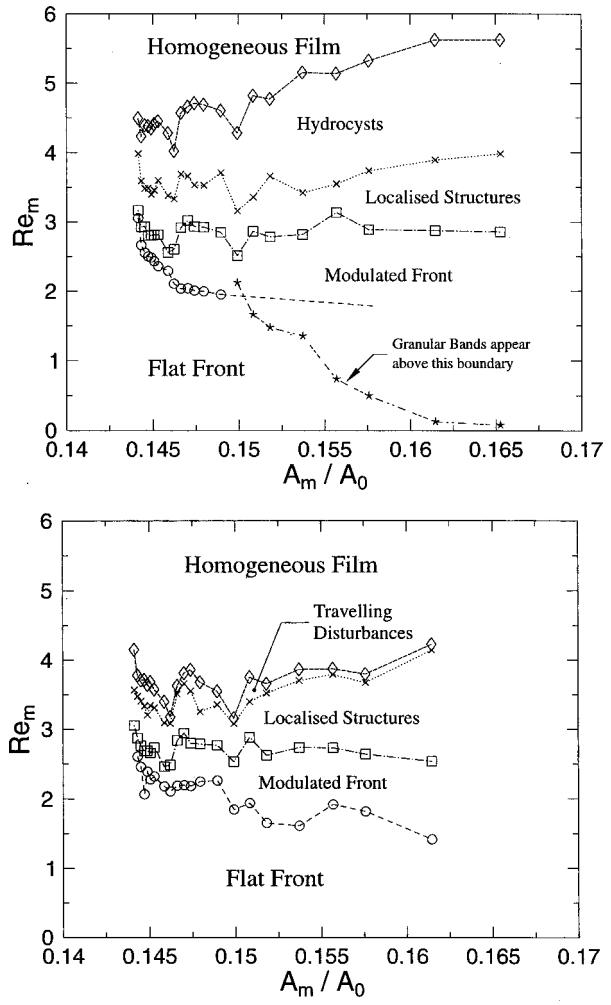

FIG. 8. Influence of increasing amounts of granular additives on the transitional Reynolds number associated with the state-transition boundaries. The data displayed were obtained after adding increasing amounts of granular additives to an initially granule-free system with a filling fraction of $A/A_0 = A_m/A_0 = 0.144$. The rotational speed of the cylinder is (a) increased from rest, (b) decreased from initially high rotation rates by a sequence of successive small increments.

effects caused by the granular additives, as such, and those superposed effects which are simply a result of the modified filling fraction. The anticipated filling-level effects can be inferred from the data of Figs. 6(a), 6(b), and Fig. 7. Nevertheless, Fig. 8 reveals that there is a marked effect of the granular additives on the state-transition boundary between the flat-front and the modulated-front state. Figures 8(a) and 8(b) show that the critical rotational velocity at which this transition occurs decreases. With reference to Fig. 6(a) this velocity is, however, expected to increase if the change was simply a result of an increased filling fraction. Consequently the observed drop in the critical transition velocity for $A_m/A_0 \leqslant 0.15$ is a consequence of the granules affecting the fluid dynamics and not a result of the associated change of the filling fraction.

Above $A_m/A_0 = 0.15$ granule bands form. As discussed in Sec. III B, it was then not possible to decide whether the onset of the modulated-front state coincides with band formation or whether the bands initiate the development of a different type of modulated front. This is reflected in Fig. 8(a) through the line initially represented by circles for $A_m/A_0 < 0.15$ and continued for $A_m/A_0 \geqslant 0.15$ by stars. The continuation of the line marked by the circles into the region of $A_m/A_0 \geqslant 0.15$ is an extrapolation based on the slope suggested by the data points in the region just below $A_m/A_0 = 0.15$.

Figure 8 further shows that the velocity interval over which the modulated-front state is observed is significantly broadened by increasing amounts of granular additives. In the granule-free system the modulated front is only observed over a very narrow Reynolds-number interval and in a very narrow regime of filling fractions as was revealed by the discussion of the results shown in Fig. 6(a). It was emphasized above that it is not a simple matter to adjust the system parameters such that a modulated front is displayed by the granule-free system. In the rimming flow containing granular additives, however, it is not at all difficult to tune the system into a modulated-front state. In this sense the influences of granular additives can, thus, be interpreted as having a strong stabilizing effect on the modulated-front state.

The remaining state-transition boundaries appear to be less strongly influenced by the addition of granular material. Considering the ambiguity which arises from filling-level effects and which is associated with the data representation in Figs. 8(a) and 8(b) it does not seem appropriate to attempt to comment in detail on these boundaries. Nevertheless, there appears to be slight drop in the critical transition velocity from the modulated-front state to the regime displaying localized structures as well as for the transition from the localized-structure regime to the regime showing hydrocysts. If this drop is indeed significant then it has to be attributed, for the same reasons as above, to the granules affecting the dynamics of the system rather than to a modification of the filling fraction.

A similar behavior as in the case of increasing cylinder velocities is observed for the corresponding state-transition boundaries in the case of decreasing cylinder velocities. A comparison of corresponding boundaries in Figs. 8(a) and 8(b) reveals, similar to the granule-free case, relatively pronounced hysteresis effects for the stability boundary of the homogeneous-film state. The remaining boundaries show less appreciable hysteresis effects.

We will now obtain some quantitative information concerning the physics responsible for changes of the locations of the state-transition boundaries. In Sec. III B it was described that the granules remain uniformly distributed throughout the fluid for lower granule concentrations. Under these conditions the granules will not significantly affect the surface tension of the silicone fluid. It thus appears reasonable to assume that influences on the transition boundaries between two flow states should be reflected only through effects arising from the competition between an increased bulk viscosity and an increased bulk density of the fluid. This competition can be studied and quantified by considering the effects of granule addition on the value of the parameter Λ. We assume that Λ remains the appropriate parameter to characterize the ratio of viscous stresses and gravitational forces as long as the granule concentration remains below the criti-

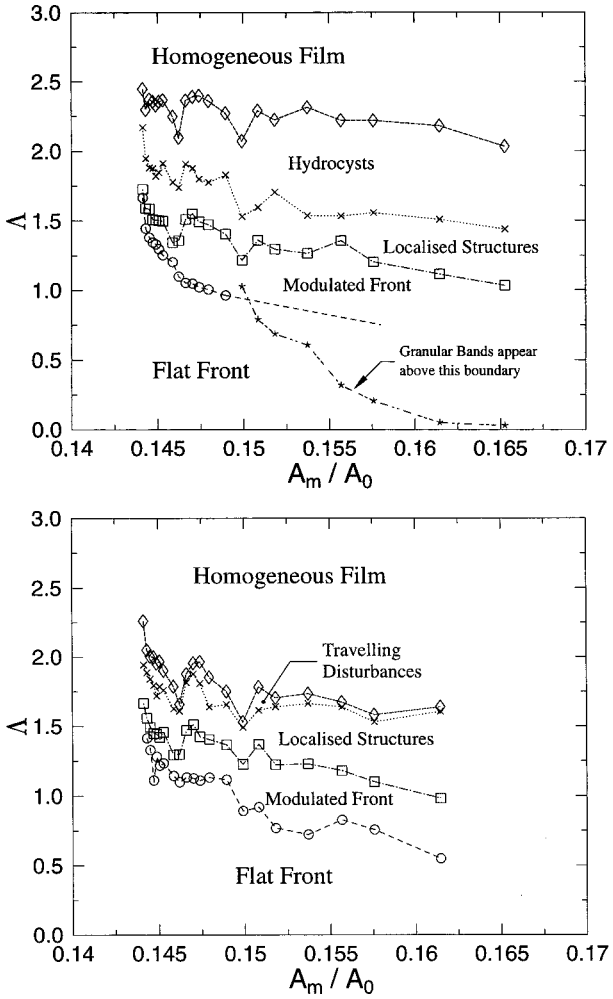

FIG. 9. Influence of increasing amounts of granular additives on the parameter Λ associated with the state-transition boundaries. The data displayed were obtained after adding increasing amounts of granular additives to an initially granule-free system with a filling fraction of $A/A_0=A_m/A_0=0.144$. The rotational speed of the cylinder is (a) increased from rest (b) decreased from initially high rotation rates by a sequence of successive small increments.

cal value of $M_c \approx 0.12\,\mathrm{g\,cm^{-3}}$ above which granule-band formation is observed.

For a granule-free system the value of Λ was expected to be constant along each state-transition boundary in the plane displaying ω_c as a function of A^2. This was confirmed to be correct by our experimental data displayed in Fig. 7 for filling levels with $A^2 \leqslant 200\,\mathrm{cm}^4$ (corresponding to filling fractions $A/A_0 \leqslant 0.18$). As long as the filling fraction remains below $A/A_0 \leqslant 0.18$ any changes of Λ, which follow the addition of granules to the system, consequently indicate how the ratio of viscous stresses and gravitational forces at the point of transition has been affected for the particular state transition considered.

Figures 9(a) and 9(b) display the value of Λ as a function of the modified filling fraction A_m/A_0 for the data of Figs. 8(a) and 8(b). With respect to our above discussion we expect Λ to be independent of A_m/A_0 along each state-transition boundary as long as $A/A_0=A_m/A_0<0.18$. Figures 9(a) and 9(b) show that the value of Λ decreases with increasing amounts of granular additives for all of the displayed state-transition boundaries. With regard to the physical interpretation of Λ it can consequently be concluded that the addition of granular material appears to result in more pronounced effects on the gravitational forces then on the viscous stresses. This suggests that the observed effects of granular additives on the locations of the state-transition boundaries in question are mainly a consequence of a modification of the bulk density of the fluid rather then of a modification of its bulk viscosity. This is the main result of this study.

IV. SUMMARY AND CONCLUSIONS

We have experimentally investigated the rimming flow established inside a partially fluid-filled cylinder which rotates around a horizontal axis of rotation. For the first time effects of granular additives on transition boundaries between certain flow states adopted by the fluid in the cylinder have been studied. For the granule-free flow we have essentially corroborated the results of previous authors. We have confirmed that for the investigated state transitions the ratio of viscous stresses and gravitational forces remains constant along each state-transition boundary as long as the filling level of the cylinder is below a certain critical level. For higher filling levels, however, our new data suggest that gravitational forces start to become increasingly more important.

Our experiments concerned with the influence of granular additives on the flow have shown that state transitions remain qualitatively similar to those in the granule-free system as long as the granule concentration is below some critical level. Nevertheless, it was found that even small granule concentrations can have a significant influence on the actual transition boundaries. Granular additives can lead to the stabilization of certain flow states and to an increased parameter range over which states can be observed. In particular it was found that the effects on the investigated transition boundaries appear to be due to an increased bulk density associated with increasing granule concentrations of the solid–liquid flow.

For higher granule concentrations an apparent qualitative change in the flow structure was observed to occur. This change was reflected in the formation of a pattern of equally-spaced circumferential granular bands on the inner cylinder wall. These bands form as a consequence of the accumulation of particulate material at certain positions along the span of the cylinder. This pattern has apparently not been previously documented in the literature for the flow studied here. It was observed that the wavelength of the band pattern is independent of the granule concentration and that it increases with the angular velocity of the cylinder. It was concluded that the pattern is probably formed as a result of shear-induced migration/diffusion.[23]

We are currently planing a more systematic study of the effects of granular additives on state-transition boundaries of rimming flows. The planned experimental program will investigate comprehensive parameter ranges for the fluid density and its viscosity as well as for the particle size, density,

and shape. It is anticipated that this study will also facilitate the investigation of underlying scaling relations for the effects of granular additives on the state-transition boundaries.

We conclude this paper with a brief comment concerning a consequence of our results on a more general topic. Our experiments have shown that even small concentrations of granules in the fluid can have a significant influence on state-transition boundaries. Hence, our results bear relevance with regard to issues associated with the suitability of certain flow-measurement techniques for studies such as the one described here. Our results demonstrate that the suitability of techniques relying on tracer particles (such as Laser Doppler Anemometry or Particle Image Velocimetry) might be restricted whenever the focus of interest is on the dynamics of the granule-free flow.

[1]F. Melo, ''Localized states in a film-dragging experiment,'' Phys. Rev. E **48**, 2704 (1993).
[2]F. Melo and S. Douady, ''From solitary waves to static patterns via spatiotemporal intermittency,'' Phys. Rev. Lett. **71**, 3283 (1993).
[3]D. P. Vallette, W. S. Edwards, and J. P. Gollub, ''Transition to spatiotemporal chaos via spatially subharmonic oscillations of a periodic front,'' Phys. Rev. E **49**, R4783 (1994).
[4]D. P. Vallette, G. Jacobs, and J. P. Gollub, ''Oscillations and spatiotemporal chaos of one-dimensional fluid fronts,'' Phys. Rev. E **55**, 4274 (1997).
[5]T. D. Karapantsios, N. A. Tsochatzidis, and A. J. Karabelas, ''Liquid distribution in horizontal axially rotated packed beds,'' Chem. Eng. Sci. **48**, 1427 (1993).
[6]H. Benkreira, R. Patel, M. F. Edwards, and W. L. Wilkinson, ''Classification and analysis of coating flows,'' J. Non-Newtonian Fluid Mech. **54**, 437 (1994).
[7]B. I. Wilhelmsson, J. F. McKibben, S. G. Stenström, and C. K. Aidun, ''Condensate flow inside paper dryer cylinders,'' J. Pulp Pap. Sci. **21**, J1 (1995).
[8]J. W. Chew, ''Analysis of the oil film on the inside surface of an aeroengine bearing chamber,'' American Society of Mechanical Engineers, New York, Paper No. 96-GT-300, presented at the International Gas Turbine and Aeroengine Congress and Exhibition, Birmingham, UK, June 10–13 1996, p. 8 (unpublished).
[9]R. E. White, ''Residual condensate, condensate behavior, and siphoning in paper driers,'' Tech. Assoc. Pulp Paper Ind. **39**, 228 (1956).
[10]R. E. White and T. W. Higgins, ''Effect of fluid properties on condensate behavior,'' Tech. Assoc. Pulp Paper Ind. **41**, 71 (1958).
[11]O. M. Phillips, ''Centrifugal waves,'' J. Fluid Mech. **7**, 340 (1960).
[12]R. T. Balmer, ''The Hydrocyst: A stability phenomenon in continuum mechanics,'' Nature (London) **227**, 600 (1970).
[13]S. Thoroddsen and L. Mahadevan, ''Experimental study of coating flows in a partially-filled horizontal rotating cylinder,'' Exp. Fluids **23**, 1 (1997).
[14]J. Sanders, D. D. Joseph, and G. S. Beavers ''Rimming flow of a viscoelastic liquid inside a rotating horizontal cylinder,'' J. Non-Newtonian Fluid Mech. **9**, 269 (1981).
[15]A. E. Hosoi and L. Mahadevan, ''Axial instability of a free-surface front in a partially filled horizontal rotating cylinder,'' Phys. Fluids **11**, 97 (1999).
[16]S. L. Soo, *Particulates and Continuum: Multiphase Fluid Dynamics* (Hemisphere Publishing, New York, 1989).
[17]A. Einstein, ''Eine neue Bestimmung der Moleküldimensionen,'' Ann. Phys. **19**, 289 (1906).
[18]D. A. Janes, ''*A bioreactor for delicate biomaterials: Physical and process factors in plant biotechnology*,'' Ph.D. dissertation, Department of Chemical Engineering, University of Birmingham, 1988.
[19]D. A. Janes and N. H. Thomas, ''On particle motions within rotating flow annular vessels,'' in Proceedings of the Symposium on Fluid Mixing IV, organized by I. Chem. E., University of Bradford, England, 11–13 September, 1990 (unpublished), pp. 281–295.
[20]M. Tirumkudulu, A. Tripathi, and A. Acrivos, ''Particle segregation in monodisperse sheared suspensions,'' Phys. Fluids **11**, 507 (1999).
[21]M. J. Karweit and S. Corrsin, ''Observations of cellular patterns in a partly filled, horizontal, rotating cylinder,'' Phys. Fluids **18**, 111 (1975).
[22]E. Fried, A. Q. Shen, and S. T. Thoroddsen, ''Wave patterns in a thin layer of sand within a rotating horizontal cylinder,'' Phys. Fluids **10**, 10 (1998).
[23]D. Leighton and A. Acrivos, ''The shear-induced migration of particles in concentrated suspensions,'' J. Fluid Mech. **177**, 109 (1987).
[24]H. K. Moffat, ''Behavior of a viscous film on the outer surface of a rotating cylinder,'' J. Mec. **16**, 651 (1977).
[25]R. E. Johnson, ''Steady-state coating flows inside a rotating horizontal cylinder,'' J. Fluid Mech. **190**, 321 (1988).